Human ovarian cancer stem/progenitor cells are stimulated by doxorubicin but inhibited by Mullerian inhibiting substance

Katia Meirelles[a,1], Leo Andrew Benedict[a,1], David Dombkowski[b], David Pepin[a], Frederic I. Preffer[b,c], Jose Teixeira[d,e], Pradeep Singh Tanwar[d,e], Robert H. Young[c], David T. MacLaughlin[a], Patricia K. Donahoe[a,2], and Xiaolong Wei[a,2]

[a]Pediatric Surgical Research Laboratories, Department of Surgery, [b]Flow Cytometry Laboratory, [c]Department of Pathology, [d]Vincent Center for Reproductive Biology, and [e]Department of Obstetrics and Gynecology, Massachusetts General Hospital and Harvard Medical School, Boston, MA 02114

Contributed by Patricia K. Donahoe, December 20, 2011 (sent for review November 17, 2011)

Women with late-stage ovarian cancer usually develop chemotherapeutic-resistant recurrence. It has been theorized that a rare cancer stem cell, which is responsible for the growth and maintenance of the tumor, is also resistant to conventional chemotherapeutics. We have isolated from multiple ovarian cancer cell lines an ovarian cancer stem cell-enriched population marked by CD44, CD24, and Epcam (3+) and by negative selection for Ecadherin (Ecad−) that comprises less than 1% of cancer cells and has increased colony formation and shorter tumor-free intervals in vivo after limiting dilution. Surprisingly, these cells are not only resistant to chemotherapeutics such as doxorubicin, but also are stimulated by it, as evidenced by the significantly increased number of colonies in treated 3+Ecad− cells. Similarly, proliferation of the 3+Ecad− cells in monolayer increased with treatment, by either doxorubicin or cisplatin, compared with the unseparated or cancer stem cell-depleted 3−Ecad+ cells. However, these cells are sensitive to Mullerian inhibiting substance (MIS), which decreased colony formation. MIS inhibits ovarian cancer cells by inducing G1 arrest of the 3+Ecad− subpopulation through the induction of cyclin-dependent kinase inhibitors. 3+Ecad− cells selectively expressed LIN28, which colocalized by immunofluorescence with the 3+ cancer stem cell markers in the human ovarian carcinoma cell line, OVCAR-5, and is also highly expressed in transgenic murine models of ovarian cancer and in other human ovarian cancer cell lines. These results suggest that chemotherapeutics may be stimulative to cancer stem cells and that selective inhibition of these cells by treating with MIS or targeting LIN28 should be considered in the development of therapeutics.

chemotherapy with cisplatin | pluripotency factors

Cancer stem cells for a number of different malignancies (1–4) are capable of unlimited self-renewal and, when stimulated, differentiation and proliferation, which contribute to tumorigenicity, recurrence, metastasis, and drug resistance. The identification of flow cytometry-compatible markers for these stem/progenitor cells in human ovarian cancer makes feasible separation, analysis, and testing for insights into these events and for discovery of new therapeutic targets and the introduction of treatment protocols directed at stem cell targets.

Cells positive for three markers (3+)—CD44, CD24, and Epcam (5)—conserved across primary human ovarian cancers, ovarian cancer cell lines, and normal Fallopian tube fimbria showed stem cell characteristics and increased resistance to chemotherapeutic agents, yet sensitivity to Mullerian inhibiting substance (MIS) (5), a.k.a. anti-Mullerian hormone, a fetal testicular protein (6) that causes Mullerian duct regression. MIS was tested because human epithelial ovarian cancers, which recapitulate the embryonic Mullerian ducts (7), express MIS receptor type II (MISRII) in a large majority of cases (8), and human recombinant MIS inhibits their growth in vitro and in vivo (9, 10).

Because the MISRII-expressing surface epithelium of the ovary is normally characterized by expression of epithelial and mesenchymal markers (11, 12), which become predominantly mesenchymal in transgenic animals as tumor initiation occurs (13), we refined the 3+ population in ovarian cancer cell lines by negative selection for Ecadherin (3+Ecad−), down-regulation of which occurs during epithelial-to-mesenchymal transformation in a variety of cancers (14, 15) and is also associated with poor outcome (16). This 3+Ecad− population of ovarian cancer proved to be more highly enriched than the 3+ population alone for stem/progenitor characteristics and was also resistant to chemotherapeutic agents but sensitive to MIS.

The present study found that LIN28, a microRNA (miRNA)-binding protein known to regulate expression of cell cycle-related genes and to contribute to cancer stem cell self-renewal and differentiation (17, 18), was the only pluripotency marker among those known to reprogram pluripotency in somatic cells that was increased in our cancer stem cell-enriched population (3+Ecad− separated cells). In addition, LIN28 was also increasingly expressed in transgenic mouse ovarian cancer models made more aggressive with progressive loss of *Misr2* (13). Furthermore, receptor-mediated MIS functional activity correlated with both cell cycle arrest and specific up-regulation of the cyclin-dependent kinase (CDK) inhibitor p15.

These findings make it mandatory to test both the stem and the nonstem population in each patient for sensitivity to chemotherapeutic agents and to biologics such as MIS when planning treatment strategies for ovarian cancer, and targeting of LIN28 may be another strategy to improve suppression of this elusive stem cell population.

Results

Triple-Positive (3+) Cells with Loss of Ecadherin (3+Ecad−) Are More Tumorigenic than Either 3+ Cells Alone or Triple-Negative Cells That Retain Expression of Ecadherin (3−Ecad+). We recently identified a CD44+, CD24+, Epcam+ (3+) population, selectable by flow cytometry, which is enriched for stem/progenitor cells (5). When combined with negative selection for Ecadherin (3+Ecad−), the resulting smaller population consistently formed more and larger colonies [Fig. 1*A*, Sloan–Kettering ovarian cancer cell line 3 (SKOV-3), *Lower* panels; Fig. 1*B*, human ovarian carcinoma cell line 5 (OVCAR-5)] than did 3+ alone (Fig. 1*A*, SKOV-3, *Upper* panels; Fig. S1) or when triple-negative (3−) cells were combined

Author contributions: K.M., L.A.B., D.P., F.I.P., D.T.M., P.K.D., and X.W. designed research; K.M., L.A.B., D.D., D.P., J.T., P.S.T., and X.W. performed research; D.D., F.I.P., J.T., P.S.T., and R.H.Y. contributed new reagents/analytic tools; K.M., L.A.B., D.D., D.P., J.T., F.I.P., D.T.M., P.K.D., and X.W. analyzed data; and K.M., L.A.B., D.P., P.K.D., and X.W. wrote the paper.

The authors declare no conflict of interest.

[1]K.M. and L.A.B. contributed equally to this work.

[2]To whom correspondence may be addressed. E-mail: pdonahoe@partners.org or xwei2@partners.org.

This article contains supporting information online at www.pnas.org/lookup/suppl/doi:10.1073/pnas.1120733109/-/DCSupplemental.

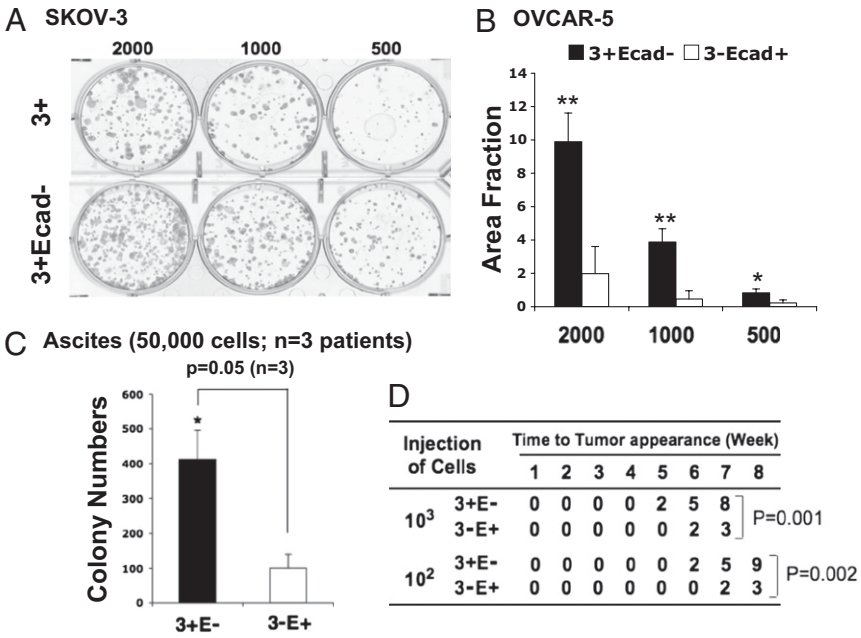

Fig. 1. Enrichment of human ovarian cancer stem cells enhances colony growth in vitro and shortens tumor-free interval in vivo. (*A* and *B*) CD44/CD24/Epcam triple-positive (3+) and 3+Ecad− cells were isolated from human ovarian cancer cell line SKOV-3 (*A*), or 3+Ecad− and 3−Ecad+ cells were separated from human ovarian cancer cell line OVCAR-5 (*B*) by FACS and plated at the indicated numbers in six-well plates. After incubation for 15 d, colonies were stained and measured. 3+Ecad− (*A*, *Lower*) formed more colonies than 3+ alone (*A*, *Upper*) (representative of $n = 3$; $^*P < 0.05$; Fig. S1). 3+Ecad− OVCAR-5 cells also grew more colonies than 3−Ecad+ cells as quantitated (*B*) as a fraction of the area of each well ($n = 3$) ($^*P < 0.05$; $^{**}P < 0.01$). (*C*) 3+Ecad− and 3−Ecad+ cells isolated from primary ascites from ovarian cancer patients were plated at 50,000 cells in low-melting agarose in 12-well plates and incubated for 2–3 wk, and then colonies were counted. 3+Ecad− formed more colonies than 3−Ecad+ when colony counts were compared in three patients ($^*P < 0.05$). (*D*) 3+Ecad− and 3−Ecad+ cells separated from OVCAR-5 were serially diluted (10^3, 10^2 cells), resuspended in 1:1 PBS/Matrigel, and injected s.c. into 5-wk-old female NOD/SCID mice (nine mice for each group). Kaplan–Meier analysis of 10^3 ($P < 0.001$) and 10^2 ($P < 0.002$) for 3+Ecad− compared with 3−Ecad+ cells shows a significant difference in time to tumor appearance (tumor-free interval). Tick bars indicate SD.

with positive selection of Ecadherin (3−Ecad+) (Fig. 1*B*, OVCAR-5), suggesting that the absence of Ecadherin contributes to the enrichment of the stem population. We also found that the 3+Ecad− population separated from human primary ovarian cancer ascites formed more colonies than did 3−Ecad+ populations (Fig. 1*C*). Enrichment of 3+ OVCAR-5 cells with negative selection for Ecadherin (3+Ecad−) also led to earlier tumor appearance (shorter latency) when 10^3 or 10^2 cells were injected into the right flank of non-obese diabetic (NOD)/SCID mice compared with 3− cells, with positive expression of Ecadherin (3−Ecad+) as a control, injected into the left flank (Fig. 1*D* and Fig. S2). The 3+Ecad− cells also grew larger tumors after injection of 10^2 cells than did the same number of 3−Ecad+ cells (Fig. S3) when measured at 8 wk. The histology characterizing OVCAR-5 tumors, whether 3+Ecad− or 3−Ecad+, was that of a highly malignant serous cystadenocarcinoma with signet cells and multicystic components (Fig. S4) (19).

MIS Inhibits Whereas Doxorubicin Stimulates Colony and Monolayer Growth of the Stem Cell-Enriched Population (3+Ecad−). Although we previously found by flow cytometry that the ratio of the 3+ cells to total cells increased after treatment with chemotherapeutic agents and decreased after receptor-mediated treatment with MIS (5), further separation of 3+Ecad− and 3−Ecad+ OVCAR-5 cells showed changes in absolute numbers of colonies. 3+Ecad− OVCAR-5 cells grew more colonies than did 3−Ecad+ cells (Fig. 2*A*, control; Fig. S5), which supports our previous finding in normal ovarian surface epithelium (20). However, when separated cells were treated with MIS or doxorubicin for 14 d, MIS significantly inhibited colony growth of the 3+Ecad− cells (Fig. 2*A*, *Upper* panels; Fig. 2*C*); conversely, 3+Ecad− cells were stimulated by the chemotherapeutic agent doxorubicin (Fig. 2*B*, *Upper* panels; Fig. 2*C*). Treatment of unseparated OVCAR-5 cells in monolayer with doxorubicin, which resulted in a significant inhibition in total viable cell number (Fig. 2*D*, *Left*), also decreased the 3−Ecad+ population (Fig. 2*D*, *Right*), but paradoxically increased the absolute number of the 3+Ecad− stem cells (Fig. 2*D*, *Center*). Similar results were observed after dose-dependent treatment with cisplatin (Fig. S6).

MIS Inhibition of 3+Ecad− Stem Cell-Enriched Population Correlates with Cell Cycle G1 Arrest and Induction of p15. Because cell cycle regulation is important to regulate self-renewal and proliferation, we next analyzed the comparative cell cycle distribution of 3+Ecad− and 3−Ecad+ cells after treatment with MIS or doxorubicin. MIS treatment significantly increased the percentage of 3+Ecad− OVCAR-5 cells in G1 (Fig. 2*E*, *Left*), but not that of the 3−Ecad+ OVCAR-5 cells (Fig. 2*F*, *Left*). By contrast, doxorubicin decreased the percentage of 3+Ecad− OVCAR-5 cells in G1 (Fig. 2*E*, *Right*), but did not statistically significantly affect the G1 population of 3−Ecad+ OVCAR-5 cells (Fig. 2*F*, *Right*). Doxorubicin also did not statistically affect the S and G2 distribution of either 3+Ecad− or 3−Ecad+ OVCAR-5 cells (Fig. S7). Moreover, MIS treatment specifically increased the CDK inhibitors p15 (Fig. 2*G*) and p16 (Fig. S8), tested in the Misr2-directed transgenic mouse ovarian cancer (MOVCAR-7 or -8) cells, because p15 and p16 are mutated in many human ovarian cancer cell lines (21). Conversely, doxorubicin treatment decreased p15 expression in the MOVCAR-7 or -8 cells (Fig. 2*G*). Meanwhile, MIS and doxorubicin showed a similar trend for p19 and p27, but not for p18 or p21 (Fig. S8).

MIS Activates Phosphorylation of SMAD1/5/8 in MIS Receptor-Expressing Cells. MISRII was detected by Western analysis in human OVCAR-5, IGROV-1 (Institut Gustave Roussy ovarian

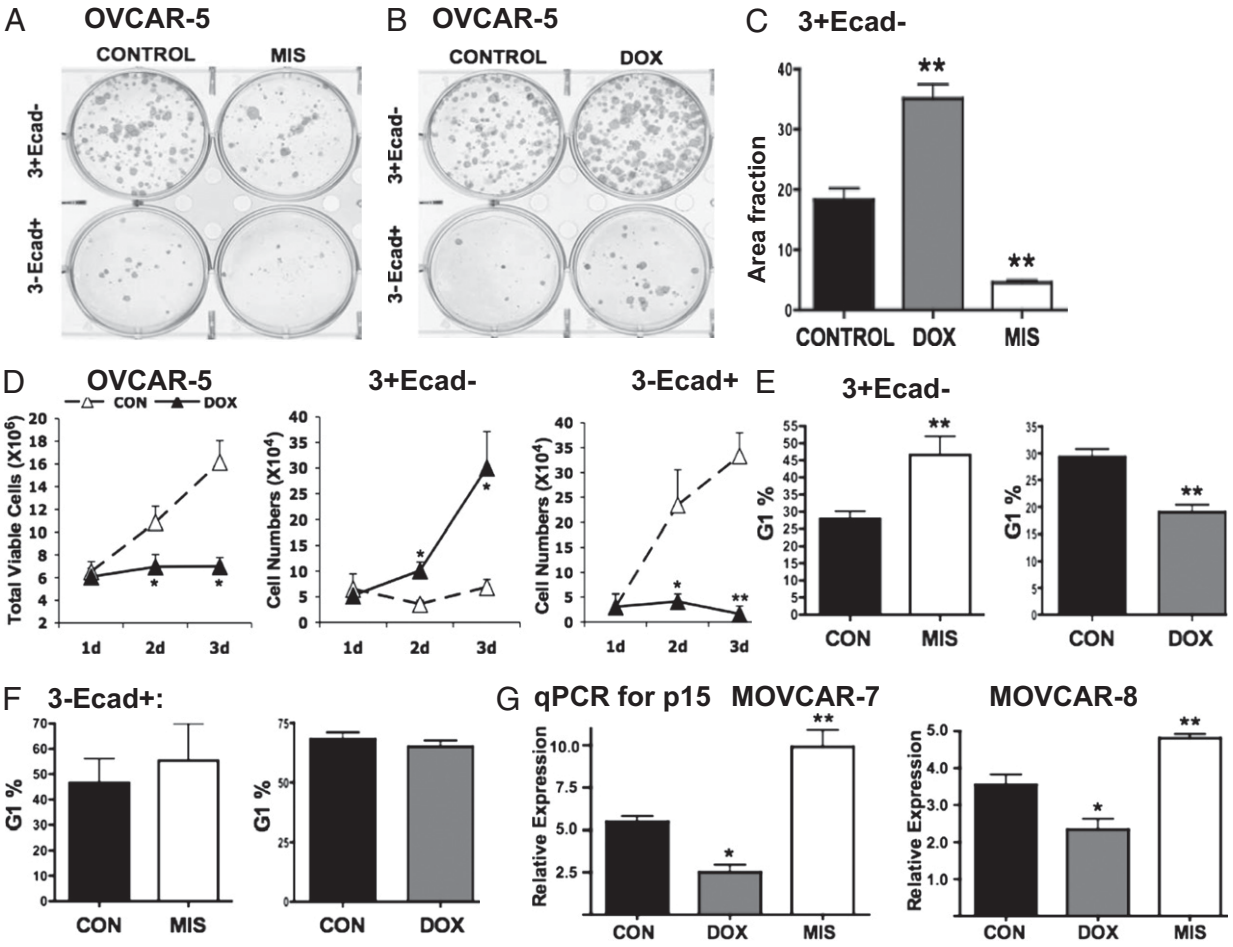

Fig. 2. MIS reduced colony formation and proliferation rate of human ovarian cancer stem cells by inducing G1 cell cycle arrest and increasing cell cycle inhibitors compared with doxorubicin. (*A–C*) 3+Ecad− and 3−Ecad+ cells isolated from OVCAR-5 by FACS were plated at 2,000 cells/well in six-well plates and treated with MIS (50 μg/mL) or doxorubicin (30 nM) or media (as a control) for 14 d. The area stained with Giemsa (*A* and *B*) was equated to colony formation (*C*) (20). The colony area formed by 3+Ecad− cells was greater than that formed by 3−Ecad+ cells (*A* and *B*, controls, and Fig. S5). MIS treatment inhibited colony formation (*A*, *Upper*, and *C*; $^{**}P < 0.01$) of the 3+Ecad− cells compared with doxorubicin (*B*, *Upper*, and *C*) ($n = 3$ separate experiments). (*D*) OVCAR-5 cells were plated at 1.6, 1.2, or 0.8×10^6 cells in T75 flasks ($n = 3$ for each cell number) and treated with doxorubicin (60 nM) for 1, 2, and 3 d. Doxorubicin treatment inhibits proliferation of total viable cells (*D*, *Left*) and 3−Ecad+ population (*D*, *Right*), but stimulates that of the 3+Ecad− population (*D*, *Center*). (*E* and *F*) In OVCAR-5 cell cycle analysis, MIS increased the 3+Ecad− cells in G1 (*E*, *Left*), whereas doxorubicin decreased 3+Ecad− in G1 (*E*, *Right*) ($n = 3$; $^{**}P < 0.01$). Neither MIS nor doxorubicin affected the G1 distribution of the 3−Ecad+ population (*F*). (*G*) MOVCAR-7 and MOVCAR-8 cell lines were treated with 50 μg/mL of MIS, 60 nM of doxorubicin, or vehicle control for 4 h. MIS increased p15 expression in MOVCAR-7 and -8 ($^{**}P < 0.01$); conversely, doxorubicin decreased p15 expression in MOVCAR-7 and -8 ($^{*}P < 0.05$).

cancer cell line), and SKOV-3 cells; in mouse MOVCAR-8 ovarian cancer cell lines (Fig. 3*A*, *Left*); and in separated 3+, 3−, 3+Ecad−, and 3−Ecad+ OVCAR-5 cells (Fig. 3*A*, *Right*). When MOVCAR-8 or OVCAR-5 cells were treated with MIS, SMAD1/5/8 phosphorylation was significantly increased (Fig. 3*B*), suggesting that MIS function is MISRII mediated, which supports previous observations (22).

Pluripotency Factor LIN28 Is Preferentially Expressed in the 3+Ecad− Stem Cell-Enriched Population. After measuring mRNAs by RT-PCR of factors known to induce pluripotency in mouse and human fibroblasts (23, 24, 25), such as *OCT3/4, NANOG, SOX2, KLF4, cMYC,* and *LIN28* (Fig. 4*A*), we found only *LIN28* to be differentially expressed in the 3+Ecad− stem cell-enriched population in OVCAR-5 xenotransplanted tumors and cell lines. LIN28 protein was strongly expressed in all five human ovarian cancer cell lines tested by Western analysis (Fig. 4*B*), whereas expression levels were lower in lines derived from normal human ovarian surface epithelium (HOSE-4 and HOSE-6). Let-7 miRNAs, which are suppressed by the miRNA-binding protein LIN28 (17, 18), were reciprocally decreased in most cancer cell lines compared with normal human surface epithelial HOSE cell lines (Fig. S9), with OVCAR-3 as an exception. Quantitative PCR (qPCR) showed higher levels of *LIN28* mRNA (Fig. 4*D*), and flow cytometry showed higher levels of LIN28 protein (Fig. 4*C*) in 3+Ecad− OVCAR-5 cells than in 3−Ecad+ or unseparated OVCAR-5 cells. Moreover, immunofluorescence showed that LIN28 colocalizes with the stem cell markers CD44 (*Left*), CD24 (*Center*), and Epcam (*Right*) (Fig. 4*E*) in human ovarian cancer OVCAR-5 cells.

***Misr2* Inactivation Correlates with Increased Lin28 Expression in Transgenic Mouse Ovarian Tumors.** We further examined expression of Lin28 in the ovarian tumors of mice in which *Misr2* Cre directed constitutively active (CA) β-catenin was overexpressed (*Misr2-Cre*$^{-/+}$;ctnnb1$^{ex3/+}$) (26). Lin28 was also examined when these transgenic mice were further crossed with *Misr2-Cre*$^{-/+}$ to inactivate the second allele of the *Misr2* (*Misr2-Cre*$^{-/-}$;ctnnb1$^{ex3/+}$). Endogenenous Lin28, normally expressed at low levels on the surface epithelium of normal ovary of the

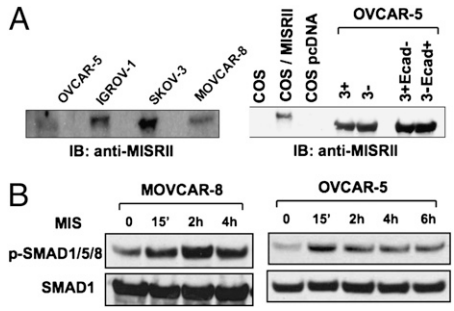

Fig. 3. MIS/MISRII activates SMAD1/5/8. (*A*) Expression of MISRII in human ovarian cancer cell lines OVCAR-5, IGROV-1, and SKOV-3 and in mouse ovarian cancer cell line MOVCAR-8 was analyzed by Western analysis with an equal amount of protein loaded in each well (*Left*). MISRII was also detected in separated 3+, 3−, 3+Ecad−, 3−Ecad+ cells of OVCAR-5 xenograft tumors (*Right*). COS (CV1 in origin and carrying SV40 genome) cells transfected with a MISRII vector or a pcDNA empty vector served as positive or negative controls (*Right*). (*B*) Immunoaffinity-purified exogenous recombinant human MIS activates SMAD1/5/8 signaling. MOVCAR-8 (*Left*) or OVCAR-5 (*Right*) cells were treated with 20 μg/mL (*Left*) or 100 μg/mL (*Right*) MIS at the indicated times, and protein was analyzed for phosphorylation of Smad1/5/8 by Western blot. Total SMAD1 protein level showed equal loading of protein (representative of $n = 3$ for each cell line).

Misr2-Cre$^{-/+}$ (Fig. 4*F*), was more differentially expressed in the malignant epithelium and in small indolent tumors of the *Misr2-Cre*$^{-/+}$;ctnnb1$^{ex3/+}$ mice (Fig. 4*G*) and more highly expressed in the ovarian tumors of the *Misr2-Cre*$^{-/-}$;ctnnb1$^{ex3/+}$ mice (Fig. 4*H*), suggesting that Misr2 expression is negatively correlated with Lin28 expression. However, no direct effect of exogenously administered MIS could be observed on either separated or unseparated populations of OVCAR-5 cells or on primary ascites, suggesting that the effect of MIS on Lin28 may be indirect (data not shown).

Discussion

We propose that, after surgical debulking and paclitaxel and platinum therapies (27, 28), additional attack of the stem cell population should improve the outcomes for this disease. Although the markers reported here enrich for a progenitor population in ovarian cancers, others such as CD133 (29) and ALDH1 (30) can produce similar enrichments. Whatever the selection panel, the practical goal is to use the markers to direct differential therapy for each patient. When ovarian cancer cell lines separated by the surface markers CD44+, CD24+, and Epcam+, (3+), further enriched by negative selection for Ecadherin (3+Ecad−), were treated with MIS, there was a significant reduction in absolute colony number and cell number; when treated with doxorubicin, these numbers paradoxically increased, indicating that there is a naive cell population with progenitor characteristics that both escapes detection and is stimulated by currently used clinical chemotherapeutics (31).

The pluripotency factor LIN28, which down-regulates the cell cycle regulator miRNA Let-7 (17, 32, 33) to cause G1 arrest and to activate cell cycle inhibitors (p15, p16) (18), is overexpressed in human ovarian cancer cell lines compared with nonmalignant HOSE-4 and HOSE-6, indicating that LIN28 correlates with malignancy. The 3+Ecad− ovarian cancer cells showed increased protein and mRNA expression of LIN28, both in vitro and in vivo, and reciprocally decreased Let-7 (32, 33). Furthermore, LIN28 coexpressed with CD44, CD24, and Epcam in OVCAR-5 cells (Fig. 4*E*). A series of transgenic mice with progressively undifferentiated ovarian carcinomas (13) expressed increasing levels of Lin28, which is normally restricted to the ovarian surface epithelium where Misr2 is coexpressed. *Misr2* inactivation correlated with up-regulation of Lin28 led us to speculate that LIN28 may contribute mechanistically, possibly via CDK inhibitors, to the differential regulation of the heterogeneous stem population of ovarian cancer cells.

MIS is a member of the TGF superfamily, which regulates cell growth, differentiation, and apoptosis by binding to MISRII,

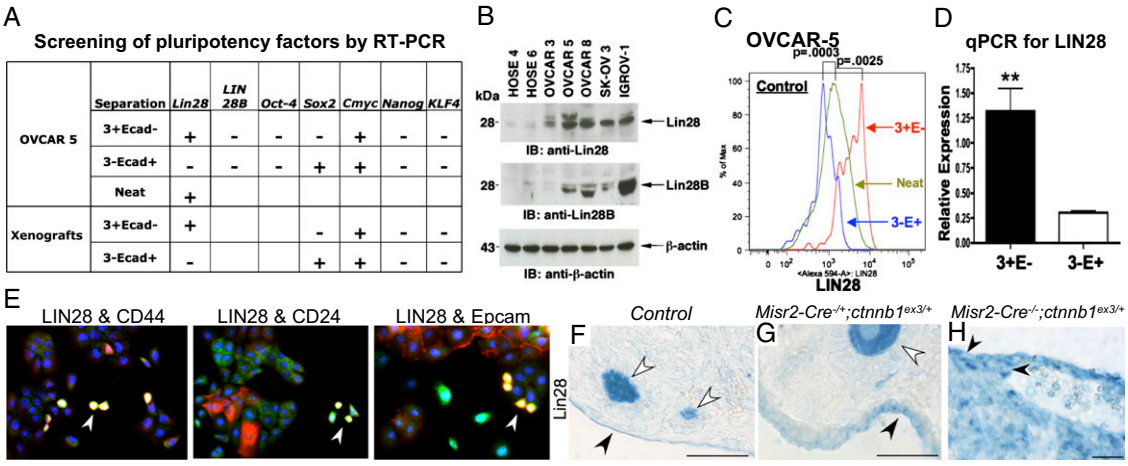

Fig. 4. Overexpression of LIN28 in 3+Ecad− stem cell-enriched population. (*A*) Total mRNAs were extracted from 3+Ecad− and 3−Ecad+ cells separated from the OVCAR-5 cell line and xenografts, and levels of mRNAs of the indicated pluripotency factors were measured by RT-PCR. *LIN28* is increased in the 3+Ecad− cells ($n = 2$ separate experiments with two sets of primers for each pluripotency factor). (*B*) Lysates from the indicated cell lines were analyzed by Western analysis with anti-LIN28/B or anti-β-actin. (*C*) Representative flow cytometry analyses of OVCAR-5 cells ($n = 3$) indicated that the 3+Ecad− subpopulation showed a statistically significant increase ($P < 0.01$) in expression of LIN28 (red peak) compared with total unseparated neat cells (green peak) or with the 3−Ecad+ population (blue peak). (*D*) qPCR of *LIN28* showed higher expression in the 3+Ecad− cells than in the 3−Ecad+ cells of OVCAR-5 ($n = 3$; $^{**}P < 0.01$). (*E*) LIN28 (green) is selectively expressed in a small number of OVCAR-5 cells where it colocalized with CD44, CD24, or EpCAM (red), suggesting that these cells (yellow cells, white arrowheads) may be cancer stem cells (representative of $n = 2$ separate experiments). (*F–H*) Lin28 immunohistochemistry of tumor tissues from transgenic mice in which *Misr2-Cre*$^{-/+}$ drives constitutively active β-catenin (*Misr2-Cre*$^{-/+}$;*ctnnb1*$^{ex3/+}$) (*G*) or in which the second *Misr2* allele is inactivated (*Misr2-Cre*$^{-/-}$;*ctnnb1*$^{ex3/+}$) (*H*). Lin28 is detectable by immunohistochemistry in the surface epithelium of the normal ovary of the Misr2-Cre$^{-/+}$ mice (*F*, black arrowhead), is up-regulated in the malignant epithelium of the *Misr2-Cre*$^{-/+}$;*ctnnb1*$^{ex3/+}$ mice (*G*, black arrowhead), and is diffusely expressed in tumors of *Misr2-Cre*$^{-/-}$;*ctnnb1*$^{ex3/+}$ mice (*H*). Germ cells serve as a positive control (white arrowheads) for comparison. (Scale bars, 100 μm in *F* and *G*; 20 μm in *H*.)

which cross-phosphorylates the tissue-specific type I receptors (12) activin-like kinase 2 (ALK2) (22, 34) or ALK3 (35), which further signal by phosphorylating SMAD1/5/8 to activate downstream pathways notable for differentiation and growth inhibition (22, 36). Activation of phospho-SMAD1/5/8 by MIS, like bone morphogenetic proteins, is correlated with G1 arrest, inhibition of CDKs (37), and activation of cell cycle inhibitors (38, 39) in breast cancer cells, which we previously observed under the influence of MIS in OVCAR-8 (40) and in breast cancer cell lines (41). When treated with MIS or doxorubicin, we found that p15 in both transgenic cell lines showed significant and opposite responses to MIS (Fig. 2*G* and Fig. S8) and doxorubicin (Fig. 2*G*), whereas the kinases tested were unaffected (data not shown).

Self-renewing normal somatic stem cells are housed in a niche, where they are slowly cycling, as illustrated by label retention (20, 42); committed progenitors, when released from the confines of a niche, undergo rapid cycling for effective expansion (43). MIS treatment resulted in G1 accumulation in the 3+Ecad− cells compared with the 3−Ecad+ population; by contrast, doxorubicin decreased the percentage of the 3+Ecad− cells in G1, indicating that the MIS may be exerting molecular effects similar to those extant in a normal niche. What we learn by comparing the same population under doxorubicin stimulation and MIS inhibition in this experimental in vitro artificial niche may allow critical molecular comparisons otherwise difficult to ascertain.

Although it has long been suspected that cancer stem cells are resistant to chemotherapeutic agents (44, 45), the present study shows that these agents actively stimulate growth of chemotherapeutic naive ovarian cancer cells and indicates that these cells require specific targeting during design of all phases of therapeutic protocols. Multidrug resistance may therefore be considered constitutive rather than therapy induced. Diagnostic and treatment paradigms will need to be individualized to include pretesting of both stem cell-enriched and stem cell-depleted populations for sensitivity of each to chemotherapeutic agents and to biologics such as MIS. Such combinations, however, together can be expected to suppress more completely the entire tumor cell population (10). Study of the separated drug-resistant population with characteristics of pluripotency will shed light on molecular mechanisms responsible for recurrence and metastases, which may in turn lead to novel drugs to target specifically this small, elusive, and insidious population. Proof of a consistent response of this population to MIS will further support its pharmaceutical development as a therapeutic in the clinic. If the poor response to chemotherapeutic agents and the favorable response to MIS and its small molecule mimetic SP600125 (5) can be repeated in the stem population isolated from a significant number of patients' primary ascites, then we can recommend that treatment of ovarian cancers should be changed to include sensitivity testing of all of the heterogeneous populations when the diagnosis is made.

Materials and Methods

Cell Lines, Chemotherapeutic Agents, and MIS. The cell lines used were maintained at the Pediatric Surgical Research Laboratories (Massachusetts General Hospital and Harvard Medical School) as previously described (4, 9, 10): HOSE-4 and HOSE-6 (a gift from Samuel Mok, Baylor College of Medicine, Houston, TX) (46), OVCAR-5 (a kind gift from Thomas Hamilton, University of Pennsylvania, Philadelphia, PA) (47), and mouse ovarian cancer MOVCAR-7 and -8 (48). Human ovarian cancer cell lines OVCAR-3 (9, 49), SKOV-3 (50), and IGROV-1 (51) were all obtained from American Type Cell Culture. Cells were treated with doxorubicin (NovaPlus), cisplatin (NovaPlus), or MIS. MIS was purified as previously described (52), and its bioactivity was assessed in embryonic Mullerian duct regression assays (53).

Harvesting of Primary Human Ovarian Cancer Ascites. Primary ascites removed therapeutically from patients with ovarian cancer at the Massachusetts General Hospital [Massachusetts General Hospital Institutional Review Board (IRB 2007P001918)] were filtered and centrifuged at 2,200 × *g* for 25 min. Cells were then resuspended in ammonium–chloride–potassium 1× buffer (Invitrogen) for 5 min to lyse red blood cells. The cells were then centrifuged at 1,500 × *g* for 5 min, lysed again if necessary, resuspended with DMEM/F-12 medium, and stored overnight at 4 °C in DMEM/F-12 for further study.

Flow cytometry and fluorescence-activated cell sorting (FACS) were performed using a seven-laser SORP LSRII or SORP 5-laser FACSVantage (BD Biosciences) as described (4, 5, 54). Human ovarian cancer cell lines or ascite cells were stained with anti-human CD24-PE, anti-mouse/human CD44-APC (allophycocyanin)/Cy7, anti-human Epcam-APC, and anti-human Ecadherin-FITC (panisotype) (Table S1) for 20 min at 4 °C. After selection for viability using 7-AAD (amino-actinomycin D) (Sigma), cells were separated for subsequent analyses. For Lin28, the cells were washed with PBS and stained with anti-mouse/human Lin28 (Primorigen Biosciences; 1:500 dilution) for 15 min at room temperature, washed, resuspended in PBS, and analyzed.

Cell Proliferation Assays. OVCAR-5 cells were seeded in T-75 flasks at different densities (1.6×10^6, 1.2×10^6, 0.8×10^6 cells) with DMEM in 10% FCS, incubated for 24 h, and then treated with either PBS (control) or 60 nM doxorubicin for 24, 48, and 72 h. Cells seeded at 0.8×10^6 were also treated with cisplatin (0.2, 0.5, 1 μM) for 72 h. Harvested total viable cells were counted by trypan blue staining in a hemocytometer and stained with anti-human CD24-PE, anti-mouse/human CD44-APC/Cy7, anti-human Epcam-APC, and anti-human Ecadherin-FITC. Flow cytometry was performed to analyze for the absolute number of 3+Ecad− and 3−Ecad+ cells, which were calculated from the total viable cell numbers by analyzing the percentage of each population adjusted for seeding density (1×, 1.5×, and 2×, respectively).

Cell Cycle Analysis. OVCAR-5 was grown to 50–60% confluency in DMEM with 10% FCS, untreated or treated with 100 μg/mL (714 nM) MIS or 60 nM doxorubicin for 48 h, harvested, and incubated with 10 μg/mL Hoechst 33342 at 37 °C for 30 min or 40 μg/mL propidium iodide (Sigma) at 25 °C for 30 min. Cells were stained with anti-human CD24-PE, anti-mouse/human CD44-APC/Cy7, anti-human Epcam-APC, and anti-human Ecadherin-FITC for 20 min at 4 °C and fixed in paraformaldehyde (1%), and the cell cycle was analyzed using the SORP LSRII.

Colony Formation Assays. Colony formation assays were performed as previously described (5). SKOV-3 or OVCAR-5 cells separated by FACS were recovered, plated on six-well plates containing 2 mL complete DMEM with 10% FCS, incubated for 14 d at 37 °C, and stained with Giemsa, and the stained area was measured as a fraction of the area of each well (Image J Rasband, National Institutes of Health; http://rsb.info.nih.gov/ij/) (20). Cells separated from primary ascites (9) were plated in agarose on 12-well (22-mm) plates (BD Biosciences) at 50,000 cells/well in 0.4% low-melting-temperature agarose (FMC BioProducts; catalog 50113) over a 0.8% layer and incubated for 2–3 wk at 37 °C. Colonies in agarose >3 ocular micrometer units were counted over a transparent gridded film with grids using a Nikon TS100 inverted microscope (100× magnification).

Western Analysis. Western analysis was performed with anti-LIN28, anti-MISRII, anti–phopho-SMAD1/5/8, anti-SMAD1, or anti–β-actin. See *SI Materials and Methods* for details.

RT-PCR. RT-PCR was performed on neat, 3+Ecad−, and 3−Ecad+ OVCAR-5 cells using a Platinum PCR SuperMix kit (Invitrogen). cDNAs were amplified using at least two primers to *LIN28, LIN28B, NANOG, SOX2, OCT4, cMYC,* and *KLF4*. For quantitative PCR, Let-7 miRNAs were extracted and analyzed from HOSE-4, HOSE-6, OVCAR-5, OVCAR-3, OVCAR-8, IGROV-1, and SKOV-3 cell lines; LIN28, p15, p16, p18, p19, p21, p27, CDK2, CDK4, and CDK6 mRNAs from OVCAR-5, MOVCAR-7, and MOVCAR-8 were measured by quantitative PCR with *GAPDH* as an internal standard. See *SI Materials and Methods* for lists of primer sequences and details. Relative expression was calculated by $2^{-\Delta Ct}$ and $2^{-\Delta\Delta Ct}$.

Immunohistochemistry and Immunofluorescence. Tissues or cultured cells were fixed in 4% paraformaldehyde and analyzed after primary (overnight at 4 °C) and secondary (1 h at room temperature) antibody incubation (Table S1) of anti-Lin28/B, anti-CD44, anti-CD24, and anti-Epcam, AlexaFluor secondary antibodies and biotinylated donkey anti-mouse or anti-rabbit antibody Fab. Images were captured with a Nikon TS2000 microscope (200× magnification) equipped with a Spot digital camera (Diagnostic Instruments).

Time to Appearance of Xenotransplanted Tumors. 3+Ecad− and 3−Ecad+ cells separated from OVCAR-5 were injected into the flanks of 5-wk-old NOD/

SCID (IRB 2009N000033/1) after serial dilution (5). After weekly monitoring, time to appearance of tumor was recorded, mice were euthanized by CO_2 inhalation, tumors were dissected and weighed, and volume (L × W × W) was measured. Fixed sections were stained with hemotoxylin and eosin for identification and comparison of tumor morphology (19).

Statistical Analysis. Univariate two-tailed *t* tests compared two sets of data having parametric characteristics in colony formation assays, cell proliferation assays, cell cycle analysis, and for Lin28 detection by flow cytometry; qPCR experiments were performed in vitro in triplicate. Kaplan–Meier and log-rank (Mantel–Cox) and Geham–Bresluw–Wilcoxan analyses were used to compare differences in time to tumor appearance between 3+Ecad– and 3–Ecad+ cells. For qPCR analysis of CDK inhibitors, nonparametric ANOVA was performed by Tukey's test. All data are expressed as means ±SD or ±SE and were analyzed using GraphPad Prism (Mac OS X, V.5.0a).

ACKNOWLEDGMENTS. We thank Ms. Caroline Coletti for editorial support; Dr. George Daley for Let-7 primers; Dr. Samuel C. Mok for HOSE-4 and -6; Dr. Denise C. Connolly for MOVCAR-7 and -8 cell lines; Scott Monsma at Primorigen for conjugated LIN28 monoclonal antibody; and Dr. Peter R. Mueller (Department of Radiology, Massachusetts General Hospital and Harvard Medical School) for providing de-identified discarded specimens from ovarian cancer patients (MGH IRB 2007P001918/6 and Dana–Farber Cancer Institute IRB 02051). These studies were supported by National Research Service Award T32 CA071345-13 (to K.M.); a Kiwanis Award from Tufts Medical Center (to L.A.B.); a Massachusetts General Hospital Executive Committee on Research Award and the Surdna-Gar Foundation (X.W.); National Institute of Child Health and Human Development Grant R01HD052701 (to J.T.); National Center for Research Resources Grants 1S10RR023440-01A1 and 1S10RR020936-01 (to F.P.); National Institutes of Health Grant R01 CA17393 (to P.K.D. and D.T.M.); the Harvard Stem Cell Institute; the Department of Defense Ovarian Cancer Research Program; the Julie Fund (P.K.D.); and gifts from Commons Development, the McBride Family Foundation, and the Austen Foundation.

1. Al-Hajj M, Wicha MS, Benito-Hernandez A, Morrison SJ, Clarke MF (2003) Prospective identification of tumorigenic breast cancer cells. *Proc Natl Acad Sci USA* 100: 3983–3988.
2. Bapat SA, Mali AM, Koppikar CB, Kurrey NK (2005) Stem and progenitor-like cells contribute to the aggressive behavior of human epithelial ovarian cancer. *Cancer Res* 65:3025–3029.
3. Reya T, Morrison SJ, Clarke MF, Weissman IL (2001) Stem cells, cancer, and cancer stem cells. *Nature* 414(6859):105–111.
4. Szotek PP, et al. (2006) Ovarian cancer side population defines cells with stem cell-like characteristics and Mullerian Inhibiting Substance responsiveness. *Proc Natl Acad Sci USA* 103:11154–11159.
5. Wei X, et al. (2010) Mullerian inhibiting substance preferentially inhibits stem/progenitors in human ovarian cancer cell lines compared with chemotherapeutics. *Proc Natl Acad Sci USA* 107:18874–18879.
6. Josso N (1973) In vitro synthesis of Müllerian-inhibiting hormone by seminiferous tubules isolated from the calf fetal testis. *Endocrinology* 93:829–834.
7. Scully RE (1977) Ovarian tumors. A review. *Am J Pathol* 87:686–720.
8. Song JY, et al. (2009) The expression of Müllerian inhibiting substance/anti-Müllerian hormone type II receptor protein and mRNA in benign, borderline and malignant ovarian neoplasia. *Int J Oncol* 34:1583–1591.
9. Masiakos PT, et al. (1999) Human ovarian cancer, cell lines, and primary ascites cells express the human Mullerian inhibiting substance (MIS) type II receptor, bind, and are responsive to MIS. *Clin Cancer Res* 5:3488–3499.
10. Pieretti-Vanmarcke R, et al. (2006) Mullerian Inhibiting Substance enhances subclinical doses of chemotherapeutic agents to inhibit human and mouse ovarian cancer. *Proc Natl Acad Sci USA* 103:17426–17431.
11. Auersperg N, et al. (1999) E-cadherin induces mesenchymal-to-epithelial transition in human ovarian surface epithelium. *Proc Natl Acad Sci USA* 96:6249–6254.
12. Zhan Y, et al. (2006) Müllerian inhibiting substance regulates its receptor/SMAD signaling and causes mesenchymal transition of the coelomic epithelial cells early in Müllerian duct regression. *Development* 133:2359–2369.
13. Tanwar PS, et al. (2009) Constitutive activation of beta-catenin in uterine stroma and smooth muscle leads to the development of mesenchymal tumors in mice. *Biol Reprod* 81:545–552.
14. Kalluri R, Weinberg RA (2009) The basics of epithelial-mesenchymal transition. *J Clin Invest* 119:1420–1428.
15. Onder TT, et al. (2008) Loss of E-cadherin promotes metastasis via multiple downstream transcriptional pathways. *Cancer Res* 68:3645–3654.
16. Uchikado Y, et al. (2005) Slug expression in the E-cadherin preserved tumors is related to prognosis in patients with esophageal squamous cell carcinoma. *Clin Cancer Res* 11: 1174–1180.
17. Heo I, et al. (2008) Lin28 mediates the terminal uridylation of let-7 precursor microRNA. *Mol Cell* 32:276–284.
18. Viswanathan SR, Daley GQ (2010) Lin28: A microRNA regulator with a macro role. *Cell* 140:445–449.
19. Che M, et al. (2001) Ovarian mixed-epithelial carcinomas with a microcystic pattern and signet-ring cells. *Int J Gynecol Pathol* 20:323–328.
20. Szotek PP, et al. (2008) Normal ovarian surface epithelial label-retaining cells exhibit stem/progenitor cell characteristics. *Proc Natl Acad Sci USA* 105:12469–12473.
21. Bandera CA, Tsui HW, Mok SC, Tsui FW (2003) Expression of cytokines and receptors in normal, immortalized, and malignant ovarian epithelial cell lines. *Anticancer Res* 23: 3151–3157.
22. Clarke TR, et al. (2001) Müllerian inhibiting substance signaling uses a bone morphogenetic protein (BMP)-like pathway mediated by ALK2 and induces SMAD6 expression. *Mol Endocrinol* 15:946–959.
23. Takahashi K, Yamanaka S (2006) Induction of pluripotent stem cells from mouse embryonic and adult fibroblast cultures by defined factors. *Cell* 126:663–676.
24. Yu J, et al. (2007) Induced pluripotent stem cell lines derived from human somatic cells. *Science* 318:1917–1920.
25. Park IH, Lerou PH, Zhao R, Huo H, Daley GQ (2008) Generation of human-induced pluripotent stem cells. *Nat Protoc* 3:1180–1186.
26. Tanwar PS, et al. (2010) Focal Mullerian duct retention in male mice with constitutively activated beta-catenin expression in the Mullerian duct mesenchyme. *Proc Natl Acad Sci USA* 107:16142–16147.
27. Matulonis UA, et al. (2008) Phase II study of carboplatin and pemetrexed for the treatment of platinum-sensitive recurrent ovarian cancer. *J Clin Oncol* 26:5761–5766.
28. Morgan RJ, Jr., et al.; National Comprehensive Cancer Network (2008) Ovarian cancer. Clinical practice guidelines in oncology. *J Natl Compr Canc Netw* 6:766–794.
29. Curley MD, et al. (2009) CD133 expression defines a tumor initiating cell population in primary human ovarian cancer. *Stem Cells* 27:2875–2883.
30. Landen CN, Jr., et al. (2010) Targeting aldehyde dehydrogenase cancer stem cells in ovarian cancer. *Mol Cancer Ther* 9:3186–3199.
31. Sharma SV, et al. (2010) A chromatin-mediated reversible drug-tolerant state in cancer cell subpopulations. *Cell* 141(1):69–80.
32. Büssing I, Slack FJ, Grosshans H (2008) let-7 microRNAs in development, stem cells and cancer. *Trends Mol Med* 14:400–409.
33. Krogan NJ, et al. (2004) High-definition macromolecular composition of yeast RNA-processing complexes. *Mol Cell* 13:225–239.
34. Visser JA, et al. (2001) The serine/threonine transmembrane receptor ALK2 mediates Müllerian inhibiting substance signaling. *Mol Endocrinol* 15:936–945.
35. Jamin SP, Arango NA, Mishina Y, Hanks MC, Behringer RR (2002) Requirement of Bmpr1a for Müllerian duct regression during male sexual development. *Nat Genet* 32: 408–410.
36. Massagué J, Wotton D (2000) Transcriptional control by the TGF-beta/Smad signaling system. *EMBO J* 19:1745–1754.
37. Alarcón C, et al. (2009) Nuclear CDKs drive Smad transcriptional activation and turnover in BMP and TGF-beta pathways. *Cell* 139:757–769.
38. Hannon GJ, Beach D (1994) p15INK4B is a potential effector of TGF-beta-induced cell cycle arrest. *Nature* 371:257–261.
39. Reynisdóttir I, Polyak K, Iavarone A, Massagué J (1995) Kip/Cip and Ink4 Cdk inhibitors cooperate to induce cell cycle arrest in response to TGF-beta. *Genes Dev* 9:1831–1845.
40. Ha TU, et al. (2000) Mullerian inhibiting substance inhibits ovarian cell growth through an Rb-independent mechanism. *J Biol Chem* 275:37101–37109.
41. Segev DL, et al. (2000) Mullerian inhibiting substance inhibits breast cancer cell growth through an NFkappa B-mediated pathway. *J Biol Chem* 275:28371–28379.
42. Kobielak K, Stokes N, de la Cruz J, Polak L, Fuchs E (2007) Loss of a quiescent niche but not follicle stem cells in the absence of bone morphogenetic protein signaling. *Proc Natl Acad Sci USA* 104:10063–10068.
43. Jung P, et al. (2011) Isolation and in vitro expansion of human colonic stem cells. *Nat Med* 17:1225–1227.
44. Gupta PB, et al. (2009) Identification of selective inhibitors of cancer stem cells by high-throughput screening. *Cell* 138:645–659.
45. Zhang S, et al. (2008) Identification and characterization of ovarian cancer-initiating cells from primary human tumors. *Cancer Res* 68:4311–4320.
46. Lau KM, Mok SC, Ho SM (1999) Expression of human estrogen receptor-alpha and -beta, progesterone receptor, and androgen receptor mRNA in normal and malignant ovarian epithelial cells. *Proc Natl Acad Sci USA* 96:5722–5727.
47. Johnson SW, Laub PB, Beesley JS, Ozols RF, Hamilton TC (1997) Increased platinum-DNA damage tolerance is associated with cisplatin resistance and cross-resistance to various chemotherapeutic agents in unrelated human ovarian cancer cell lines. *Cancer Res* 57:850–856.
48. Connolly DC, et al. (2003) Female mice chimeric for expression of the simian virus 40 TAg under control of the MISIIR promoter develop epithelial ovarian cancer. *Cancer Res* 63:1389–1397.
49. Hamilton TC, et al. (1983) Characterization of a human ovarian carcinoma cell line (NIH:OVCAR-3) with androgen and estrogen receptors. *Cancer Res* 43:5379–5389.
50. Fogh J, Wright WC, Loveless JD (1977) Absence of HeLa cell contamination in 169 cell lines derived from human tumors. *J Natl Cancer Inst* 58:209–214.
51. Bénard J, et al. (1985) Characterization of a human ovarian adenocarcinoma line, IGROV1, in tissue culture and in nude mice. *Cancer Res* 45:4970–4979.
52. Ragin RC, Donahoe PK, Kenneally MK, Ahmad MF, MacLaughlin DT (1992) Human Müllerian inhibiting substance: Enhanced purification imparts biochemical stability and restores antiproliferative effects. *Protein Expr Purif* 3:236–245.
53. Donahoe PK, Ito Y, Price JM, Hendren, WH, III (1977) Müllerian inhibiting substance activity in bovine fetal, newborn and prepubertal testes. *Biol Reprod* 16:238–243.
54. Preffer F, Dombkowski D (2009) Advances in complex multiparameter flow cytometry technology: Applications in stem cell research. *Cytometry B Clin Cytom* 76:295–314.